Diyala Journal of Engineering Sciences

Journal homepage: https://djes.info/index.php/djes

ISSN: 1999-8716 (Print); 2616-6909 (Online)

Hybrid Terrestrial -Underwater Optical Communications Link

Satea Hikmat Alnajjar[1*], Mohammed K. Al-obaidi[2], Mahmood J Ahmad[1], Baraa Munqith Albaker[2]

[1]Department of Network Engineering and Cybersecurity, College of Engineering, Al-Iraqia University, Baghdad, Iraq.
[2] Department of Electrical Engineering, College of Engineering, Al-Iraqia University, Baghdad, Iraq.

ARTICLE INFO

Article history:
Received: 24/12/2024.
Revised: 30/09/2025.
Accepted: 20/10/2025.
Available online: 10/12/2025

Keywords:

Multiple FSO/FOC
EDFA-FOC
UOWC
NLOS
Atmospheric attenuation

ABSTRACT

This study presents the design and performance evaluation of a hybrid optical communication system capable of supporting high-rate data transmission across both terrestrial and underwater environments. Conventional free-space optical (FSO) and underwater optical wireless communication (UOWC) systems have typically been investigated in isolation, limiting their applicability in scenarios requiring seamless air–water connectivity. To overcome this limitation, we propose and analyze an integrated hybrid FSO–UOWC system using OptiSystem simulations. The system incorporates an Erbium-Doped Fiber Amplifier (EDFA) to compensate for atmospheric attenuation and improve the received optical signal. Simulation results demonstrate that the proposed design significantly enhances link quality, with the received signal power improving from –29.5 dBm (without EDFA) to –5.48 dBm (with EDFA). Correspondingly, the quality factor increased from 16.18 to 60.05, ensuring reliable transmission with a bit error rate (BER) maintained below 10^{-9}. The hybrid link also supports reliable operation over water depths of up to 30 m, extending its practical applicability for marine monitoring, defense, and offshore communication networks. Compared to conventional single-medium solutions, the proposed system provides higher capacity, longer range, and improved robustness against alignment and attenuation challenges at the air–water interface. Overall, this work highlights a novel hybrid optical framework that effectively bridges terrestrial and underwater channels, offering a promising solution for next-generation broadband optical communication systems.

1. INTRODUCTION

A hybrid optical-wireless communication system is considered an important solution for the required high-speed data transmission across unexpected environmental conditions, producing unique properties such as large bandwidth scale, low latency, and inherent physical-layer security [1,4]. In underwater applications, Underwater Optical Wireless Communication (UOWC) has attracted significant interest as a cost-effective and high-bandwidth alternative to conventional acoustic systems. However, its performance is often constrained by the harsh and dynamic characteristics of the aquatic environment [5] [6]. Laboratory experiments using water tanks simulating oceanic conditions have achieved data rates of several megabits per second, highlighting UOWC's potential for a modern underwater communication system.

Compared to conventional communication systems, UOWC covers the required high data rates, besides a lower latency property by utilizing optical wavelengths to establish protected communication links, much like Free-Space Optics (FSO) systems [7,9]. Since the blue-green spectral band (450–550 nm) has very low absorption and scattering in seawater [10], recent experimental studies have examined a variety of laser and LED transmitters for UOWC applications[11]. In light of this, plenty of research has gone into creating UOWC systems that are tailored for these wavelengths [12][13]. However,

*Corresponding author's Email: sateaahn@gmail.com
DOI: 10.24237/djes.2025.18409

a number of propagation limitations affect wireless optical communication systems [14][15]. The gamma-gamma distribution is frequently used to describe the attenuation losses, misalignment, and atmospheric turbulence that impair the performance of terrestrial FSO systems [16][17]. Similar to this, UOWC linkages have to deal with water molecule absorption as well as organic matter and suspended particle scattering, which causes a great deal of route loss and temporal dispersion [18]. By altering the refractive index through changes in temperature and pressure, ocean currents exacerbate these difficulties even more. The Weibull distribution provides a good description of the changes in the received optical signal as explained in [19]-[22]. In order to facilitate high-speed, end-to-end optical connectivity across air-water barriers, this work presents an innovative communication scheme that extends optical wireless networks, taking into consideration different channel degradation variables that represent practical implementation scenarios in both terrestrial and underwater environments. The simulation is performed using OptiSystem, an integrated software platform designed for the design, simulation, and optimization of optical communication systems. It is possible to accurately depict both underwater optical wireless communication (UOWC) networks and terrestrial Free-Space Optical (FSO) networks. Because of OptiSystem has a large library of optical components and sophisticated modeling features.

This paper's remaining sections are arranged as follows: The suggested hybrid system's design is explained in Section II. The results collected are presented and discussed in Section III. The final section provides a summary of the main conclusions and recommendations for further research.

2. DESIGN OF THE HYBRID FSO–UOWC COMMUNICATION SYSTEM

This study suggests a two-layer communication channel between the terrestrial network and underwater platforms.

The terrestrial segment of the system links one side of the bidirectional FSO-2 terminal to the ground network through a hybrid FSO-1 and fiber-optic connection.

For the underwater segment, the opposing end of the FSO link—positioned on a platform above the water surface—is directed toward the sea, where the optical signal is transmitted using an optical cable to the connected underwater platforms. A multi-layer hybrid architecture, consisting of both FSO and fiber-optic components and incorporating non-line-of-sight (NLOS) optical links to submerged platforms, is depicted in Figure 1.

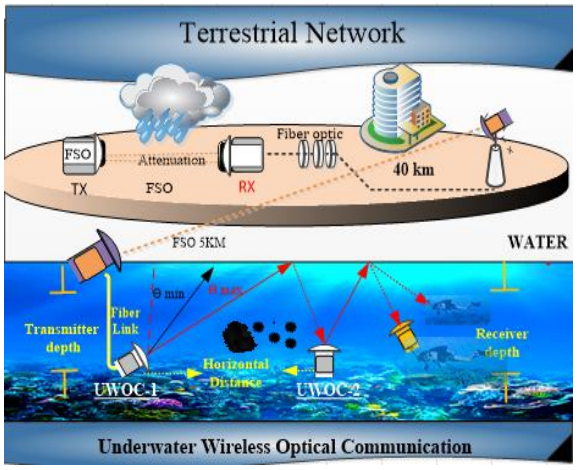

Figure 1. Underwater Optical-Terrestrial Hybrid Communications Link

This study focuses on assessing the performance of a hybrid, reconfigurable transmitter/receiver (TX/RX) free-space optical communication system integrated with optical fibers, both with and without the use of Erbium-Doped Fiber Amplifiers (EDFA), under varying weather conditions, including clear and rainy environments. It also examines how this approach enhances underwater communication quality by mitigating attenuation effects in UOWC. There are two separate layers in the suggested design. The elements of each layer, which are arranged into several steps, are shown in Figure 2.

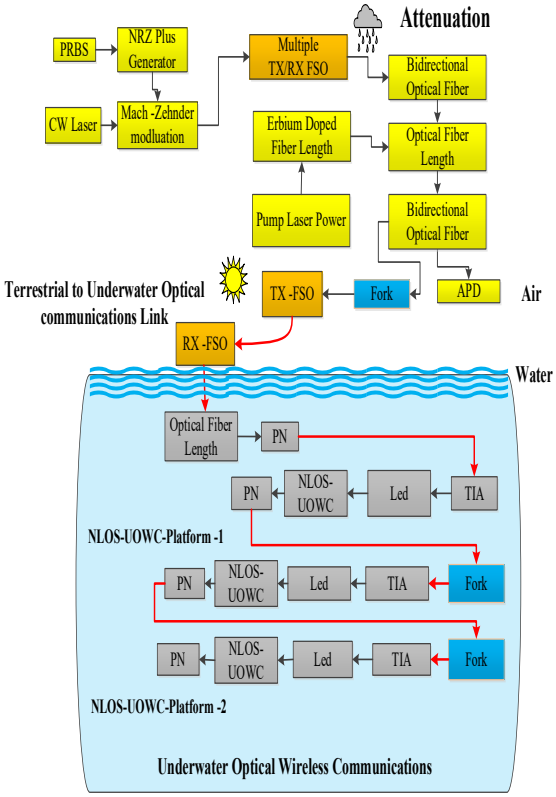

Figure 2. The Terrestrial to UOWC Configuration Systems block diagrams.

2.1 Terrestrial Optical Communication Link

This proposal employs two FSO systems: Multi TX-RX FSO-1, connected to the fiber optic link, and a second system that receives the signal from the fiber line after 40 km. Both systems are components of the hybrid configuration implemented at this level of the proposed design. It is essential to highlight the environmental degradation affecting the FSO system. A key factor in assessing signal intensity is attenuation caused by environmental variations. Signal strength is defined as the ratio between transmitted and received power. When signals propagate through a medium under different weather conditions, attenuation manifests as a reduction in signal strength [23]. The atmospheric attenuation coefficient can be calculated using the following formula:

$$\gamma(\lambda) = \frac{3.912}{v}(\lambda/550)^{q} \quad (1)$$

Here, γ, v, and λ represent visibility, particle size distribution coefficient, and wavelength, respectively, while γ denotes the attenuation coefficient. Additionally, q refers to the size distribution of scattering particles. The attenuation of the transmitted signal under various weather conditions can be modeled using q [24]. The value of q, which characterizes the relationship between visibility and atmospheric attenuation in the FSO channel, is determined based on visibility (V) as follows:

- q = 1.6 when visibility exceeds 50 km**.**
- q = 1.3 when visibility is between 6 km and 50 km**.**
- q = 0.16 × V + 0.34 when visibility ranges from 1 km to 6 km**.**
- q = V − 0.5 when visibility is between 0.5 km and 1 km**.**
- q = 0 when visibility is less than 0.5 km.

This calculation method is useful because, for a given wavelength, the attenuation depends solely on the visibility [24].

The model developed by Kim and Kruse [24] must be used to calculate the attenuation coefficient and particle size distribution. Visibility-dependent attenuation coefficients can be derived from previous calculations. According to Kim's model, the attenuation values for the FSO channel under various visibility conditions are explained in the table 1. The weather conditions impact the range and reliability of the FSO link. The supposed method will be evaluated based on these attenuation variables.

Table 1: Setting of Weather Attenuation Factor [25]-[27].

Atmospheric Attenuation		
Visibility (km)	**(1550 nm) dB/km**	**Weather**
1	10	Rain
4	2	Haze
23	0.2	Clear

Earlier models describe attenuation coefficients primarily as a function of visibility, particularly relevant to atmospheric and space-based scenarios. A typical FSO communication system consists of three fundamental elements: the transmitter, the transmission medium (FSO channel), and the receiver. The structural layout of the proposed hybrid FSO/fiber optic system is illustrated in Figure 3. An optical signal from a 1550 nm laser source, a Mach–Zehnder modulator, a pseudo-random bit sequence generator, and an NRZ pulse generator make up the transmitter [28].

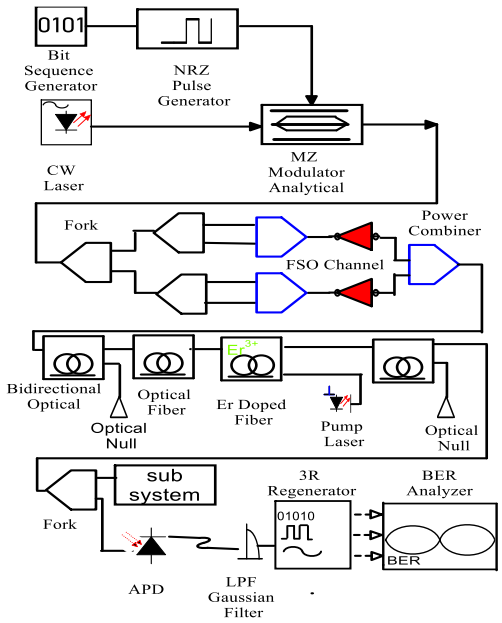

Figure 3. Simulation model of the suggested hybrid terrestrial–underwater communication link developed by OptiSystem 21

In this study, the simulation module's transmitter uses two laser arrays. Lenses are used to transmit multiple beams through various pathways. Free-space optical (FSO) communication systems can enhance link reliability under challenging weather conditions -such as fog or rain-by providing multiple transmission paths for the optical signal.

Air disturbances cause an attenuation impact on propagation beams, which differs depending on the path. The FSO channel's configuration settings are shown in Table 2.

Table 2: Configuration parameters for the proposed FSO-

1 and FSO-2 channels

Parameter	Measurement
Distance Range	500-5000 m (FSO)
Transmitter Power	-3mW
Attenuation Value	0.2 -10 dB/km
Transmitter Power diameter	25 mm
The Receiver aperture diameter	350 mm
The Beam divergence	0.001 radians
Wavelength	1.55 µm
Additional losses	1 dB

The transmitter operates at a wavelength of 1550 nm, with an optical power of –3 mW and a data rate of 1 Gb/s. A larger beam diameter lowers beam divergence. A lower divergence angle focuses the beam more tightly, allowing greater power to reach the receiver over longer distances. For this reason, the transmitter beam diameter was set at 2.5 cm. In contrast, a narrower, tighter beam is produced by a lower beam diameter, but if optics are not properly built, the beam may diverge more quickly [29]. The total number of samples, samples per bit, and sequence length are 131,072, 1024, and 128, respectively. A Bessel low-pass filter and an avalanche photodetector make up the FSO receiver module. BER and signal Q-factor are measured using a 3R regenerator. The block diagram for the hybrid multiple (TX/RX) FSO/fiber optic channel is displayed in Figure 3. By lessening the effects of signal deterioration, the employment of adaptive optical transmitters and diversity strategies, such as multiple transmission pathways, improves the durability of communication links.

Single-mode fibers of different lengths, including a 40 km fiber optic channel (FOC), are used in the terrestrial network. To further reduce dispersion over the FOC, two 3.2 km dispersion compensation fibers (DCFs) are employed [28]. A 3 m long EDFA running at 980 nm with a pumping power level of 40 mW and a noise figure of 3–6 dB compensates for attenuation in the FOC[30] .

2.2 Underwater Communications Systems

One potential technique that uses light to send data via water is underwater optical communication (UOC). Compared to traditional acoustic and radio frequency (RF) communication methods, this technique offers notable benefits such as increased bandwidth and higher data transmission speeds [31][32]. Nevertheless, the performance of underwater optical communication (UOC) systems is highly dependent on precise alignment between the transmitter and receiver. This study examines how varying angles between these components influence the communication efficiency. In the underwater layer, the optical signal enters the water upon reaching its surface, where it may be further weakened by factors such as biological interference, temperature gradients, and water properties.

Considerations for Underwater Signals

- **Attenuation:** When optical signals pass through water, they are attenuated by absorption and scattering. Signal deterioration is greatly influenced by variables like depth, water composition (such as salinity and turbidity), and biological activity**.**
- **The Function of Angle in UOC Systems:** In UOC systems, maintaining a strong and steady communication link requires exact transmitter-receiver alignment.. Misalignment due to aiming errors, dispersion, or absorption can cause significant signal loss.
- When a light beam passes between air and water, it refracts at the interface. The beam bends away from the vertical as it moves from a medium with a lower refractive index (air) to one with a higher refractive index (water). When the angle of incidence reaches a specific threshold, called the critical angle, the angle of refraction approaches 90°. If the incident angle exceeds the critical angle, total internal reflection occurs, causing the light beam to reflect into the water.

Absorption factor $a(\lambda)$, scattering factor $b(\lambda)$, which determine the extinction value $c(\lambda)$, that is poses a serious problem for the underwater wireless optical communication channel [33]

$$\boldsymbol{c(\lambda)[1/m]} = [(\boldsymbol{a(\lambda)}) + (\boldsymbol{b(\lambda)})] \quad (2)$$

These standards are established based on the intrinsic optical properties of water [34]. The absorption coefficient $a(\lambda)$ and the scattering coefficient $b(\lambda)$ are defined by these inherent characteristics. Table 3 presents these factors related to a wavelength equal to 532 nm for various water categories, as reported in [35].

Table 3. Effective extinction, dispersion, and absorption for a range of water types [35]

Categories of Water	$a(\lambda)$ 1/m	$b(\lambda)$ 1/m	$c(\lambda)$ 1/m
A pure sea	4.05×10^{-2}	2.5×10^{-3}	4.3×10^{-2}
A clear ocean	1.14×10^{-1}	3.7×10^{-2}	1.51×10^{-1}
A costal ocean	1.87×10^{-1}	2.19×10^{-1}	3.98×10^{-1}

It can be investigated that the performance of the suggested system between the transmitter and the

receiver places that are not in direct line of sight because of obstructions, misalignment, or erratic transceiver orientation by using the NLOS underwater channel component. A reflecting communication architecture is made possible by the NLOS underwater channel, as seen in Figure 1. The laser transmitter produces an upward-directed light beam characterized by inner and outer divergence angles, denoted as θ_{min} and θ_{max}, respectively. The transmitter (TX) is thought to self-align and always face upward vertically. As Figure 1 shows, the light bounces off the ocean to the air surface and illuminates an annular region that is incompletely mirrored back depending on the reflectance characteristics of the media at the boundary. Some light is reflected and some is refracted, depending on the incidence angle; however, all light is reflected if the incident angle is larger than the value of the critical-angle [36].

The concepts discussed above are applied in the proposed design to estimate the incoming signal strength at the receiver. Additionally, the impact of varying the angle on signal intensity and the consequent changes in Q-factor and BER are investigated. The complementary error function (erfc) can be used to link the BER to the Q-factor [37] provides the BER formula in terms of the Q-factor:

$$BER = \frac{1}{2} erfc\left(\frac{Q}{\sqrt{2}}\right) \quad (3)$$

Where the complementary error function , erfc(x), can be determined by:

$$erfc(x) = \frac{2}{\sqrt{\pi}} \int_x^{\infty} e^{-t^2}\, dt \quad (4)$$

A lower bit error rate (BER) corresponds to a higher Q-factor, signifying improved signal quality.

The following is a summary of the fundamental elements of the UOWC system: Block diagrams of the UOWC configuration are displayed in Figure 4. The shoreline and an offshore platform 5000 meters apart are connected by bidirectional FSO-2 communication with an attenuation of 0.2 dB/km in clear weather. The signal is sent from the offshore platform's FSO-2 receiver to a fiber optic cable that is 20 meters below the surface and connects to the UOWC-1 system.

A new technique called underwater optical wireless communication uses light to send data via water. Compared to conventional radio frequency (RF) and acoustic communications, this method has several benefits, such as increased bandwidth, faster data rates, and reduced latency. A modulated LED with a laser wavelength of 532 nm is used in the UOWC-1 platform transmitter. The modulation current (input signal) in this device is proportional to the mean optical power. Practically speaking, electrical trans-modulation between bands is used in the hybrid FSO-UOWC link. An electrical signal proportional to the received optical power is output by the FSO receiver (1550 nm PIN photodiode). The UOWC transmitter is a 532 nm LED that is driven by a Transimpedance Amplifier (TIA), which rescales and amplifies this signal. By using matched impedance and gain staging, this technique preserves signal integrity while avoiding the difficulties of direct optical wavelength shifting[38]. .

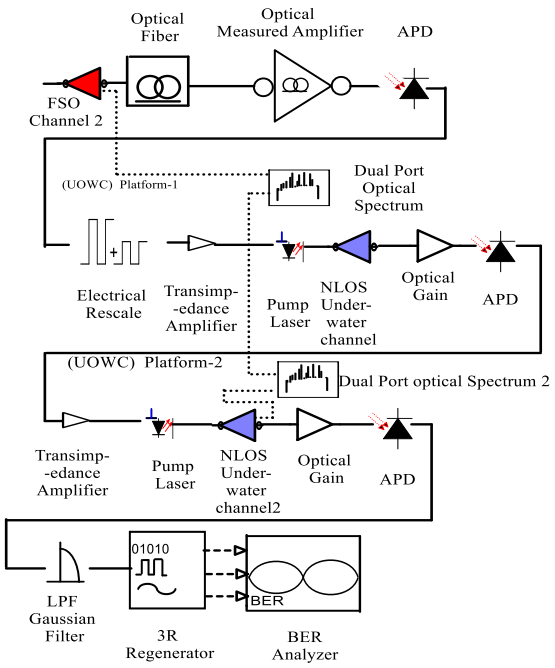

Figure 4. Simulation setup of the subsystem for the non-line-of-sight underwater optical wireless communication (NLOS-UOWC).

NLOS system, which is based on the underwater Channel-1, facilitates communication between the transmitter point and the PIN photodiode receiver point when the transmitter is not aligned with the receiver due to physical obstacles, misalignment, or non-ideal transceiver orientations. In this setup, the transmitter directs a laser beam toward the water surface at an angle exceeding the critical angle (θ_{max}). The properties of changing the angles between the transmitter and the receiver are examined in this study. A light beams with inner and outer angles (θ_{min} and θ_{max}) are emitted by transceivers that are oriented vertically upward. Fresnel's law states that at interfaces between media having varying refractive indices, propagating light is partially refracted and partially reflected. Thus, the sea surface partially reflects the light beam that is transmitted from

depth h.

The received power in the configured underwater optical communication system can be calculated using the following equation, as described in [39][40]:

$$Aann = (6.2832) \times (h + x)\ 2\ [A - B] \quad (5)$$

Where A= $cos(\theta min)$, B= $cos(\theta max)$

Generated signal from NLOS system through underwater channel-1 is communicated to the second station via the NLOS underwater channel-2, preserving its original characteristics. Table 4 summarizes the parameters used to model the NLOS underwater channels within the simulated environment. Based on these parameters, the Following section presents determined results assessing the Q-factor indicator and bit error rate (BER) of the bidirectional multiple (TX/RX) in Free-Space Optical (FSO), besides fiber optic channels (FOC).

Table 4. Numerical Parameters for the NLOS Undersea Channel

Parameter	Measurement
Wavelength value	0.532 μm
Temperature value	10 C°
Salinity percentage	3.5 %
air refraction	1.0003
Attenuation category	Pure
$a(\lambda)$	4.05×10^{-2} m^{-1}
$b(\lambda)$,	2.5×10^{-3} m^{-1}
TX depth value	(10, 20) m
RX depth value	(10, 20) m
Horizontal distance	(10, 20) m
θ_{min}	0°- 100°
θ_{max}	68°
Surface incident angle	0°

3. RESULTS AND DISCUSSION

An optimal performance for the multiple (TX/RX) FSO system can be achieved under clear weather conditions. Its effectiveness is further assessed across a range of environmental scenarios. To ensure the accuracy of our results, the system performance was validated by comparison with Kim's model and other established references before proceeding to analyze the impact of varying angles, depths, and characteristics of the NLOS underwater channel. To assess the efficiency of the proposed system, we analyze:

- Testing the system without an EDFA in the fiber optic channel (FOC) for terrestrial communications.
- Investigating attenuation under clear weather (0.2 dB/km) by varying the bidirectional FSO-2 distance, while FSO-1 remains fixed at 1000 m with 10 dB/km attenuation in rainy conditions.
- Monitoring variations in the NLOS underwater channel platforms.

Figure 5(a) illustrates a significant enhancement in received power within the FSO/Optical Fiber network when EDFA amplification is applied, with signal strength improving from –29.5 dBm to –5.48 dBm. Similarly, the Q-factor, as shown by the BER analyzer in Figure 5(b), increased markedly from 16.18 to 60.06.

After verifying the improved signal quality in the terrestrial network, its impact on extending the FSO-2 transmission range under clear weather conditions was assessed by connecting it to an underwater station through a cable length equal to 20 m. The minimum BER achievable at submerged platforms plays a crucial role in determining the allowable installation distance for FSO-2 systems on surface platforms. These results are illustrated in Figure 6, Platform-1 records a BER as low as 7.89×10^{-11} at 575 m from the transmitter, while Platform-2 records a BER of 2.73×10^{-9} at 275 m.

As a result of this enhancement, the underwater platforms showed improved performance consistent with the terrestrial network gains, as illustrated in the above figure. The second platform achieved a BER equal to 5.52×10^{-9} with a distance equal to the first platform, while the UOWC first platform reached a minimum BER of 1.44×10^{-22} at 6500 meters. Extending the FSO-2 range from 575 meters to 6500 meters provides greater flexibility for system deployment on the ocean surface. It is also noteworthy that under rainy conditions, the FSO-1 system maintains a fixed range of 1000 meters with consideration of the attenuation factor equal to 10dB/Km.

The evaluation utilized the setting parameters for both underwater stations, as tabulated in Table 5.

Table 5. Setting Applied in UOWC NLOS-1 and NLOS-2 Channel Modeling

Parameter	Measurement	
Attenuation category	Pure	
a(λ)	0.0405	1/m
b(λ)	0.0025	1/m
Tx depth value	20	m
RX depth value	20	m
Supposed horizontal distance	25	m
Inner angle	0	deg.
Outer angle	68	deg.

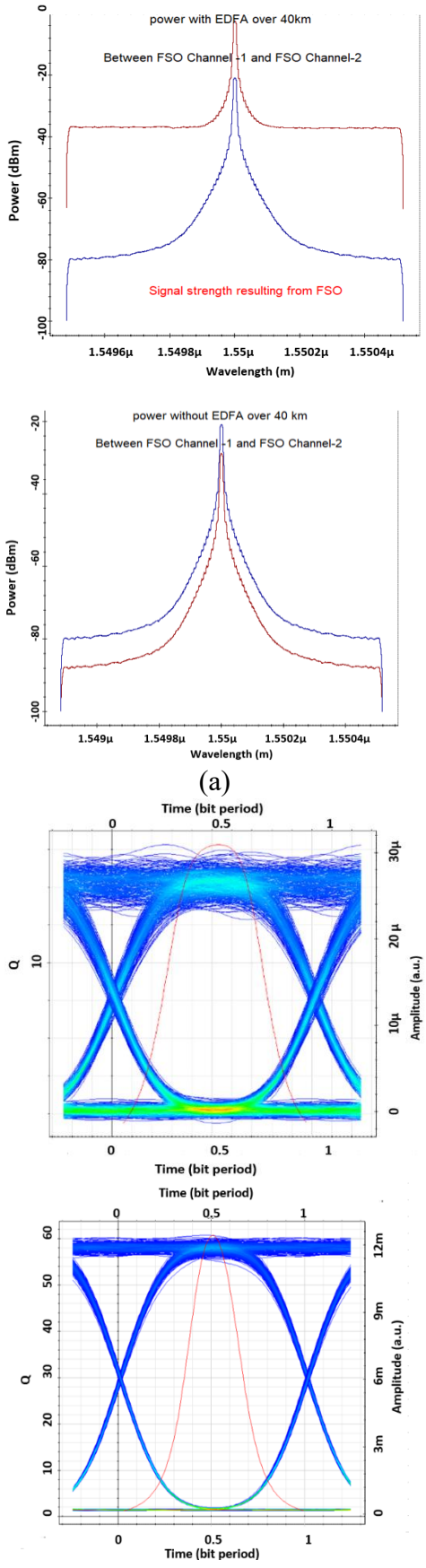

Figure 5. Ground station (FSO/Optical Fiber) performance in terms of (a) power and (b) bit error rate (BER), with and without EDFA.

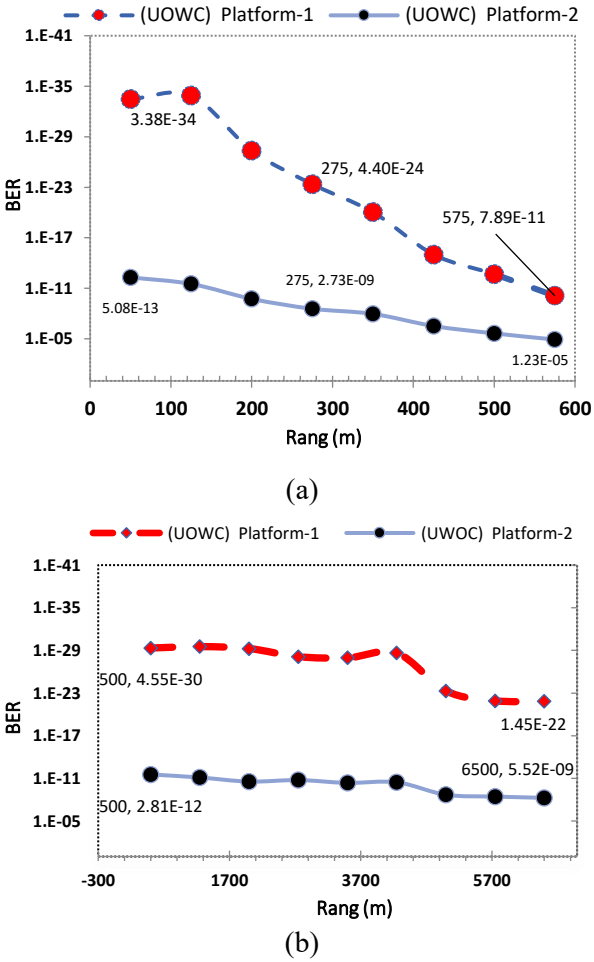

Figure 6. Behavioral responses of UOWC platforms for FSO-2 in clear water: (a) with EDFA, and (b) without EDFA

Following the network enhancement analysis, critical parameters such as incidence angles, diving depth, and the horizontal separation between the transmitter and receiver—are examined to assess their influence on the performance of the underwater platform. The lower curve in Figure 6(a) illustrates the UOWC NLOS-2 bit error ratio of 2.02×10^{-9}, which is the consequence of setting the FSO-2 bidirectional transmitter-receiver range to 5000 meters for this test. This number is typically regarded as being around the lowest permitted BER for communication applications.

Analyzing the impact of different characteristics, such as inner and outer angles, horizontal distance, and transmitter and receiver depth, comes next. At a depth of 20 meters, the transmitter and receiver's absorption coefficients (a and b) for pure seawater are 0.0405 m-1 and 0.0025 m-1, respectively.

To calculate the horizontal distance when the outer angle (θ_{max}) is 68°, signal attenuation due to absorption and scattering can be applied using parameters from Table 5. Since the vertical distance

between the transmitter and receiver is zero (i.e., both are at the same depth), the analysis primarily considers the horizontal distance using the outer angle, as described in [27], while the attenuation factor α can be calculated as:

$$\alpha = a + b = 0.0430\ 1/\text{m}\alpha \quad (6)$$

The operative range is determined by the following equation:

$$H = R \cdot tan\ (\theta max) \quad (7)$$

Where variable R equals α^{-1}, and H refers to the horizontal distance for the given parameters in a pure sea category equal to 57.63 m.

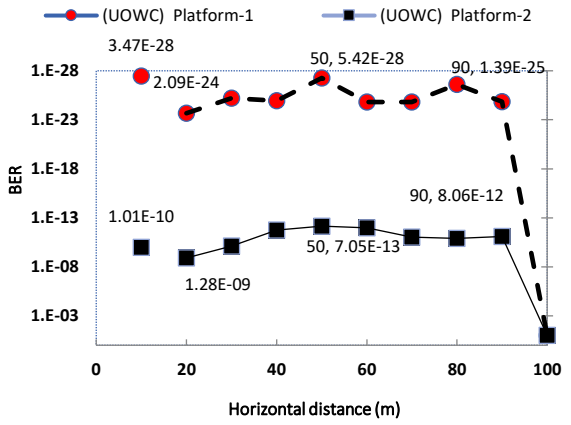

(a)

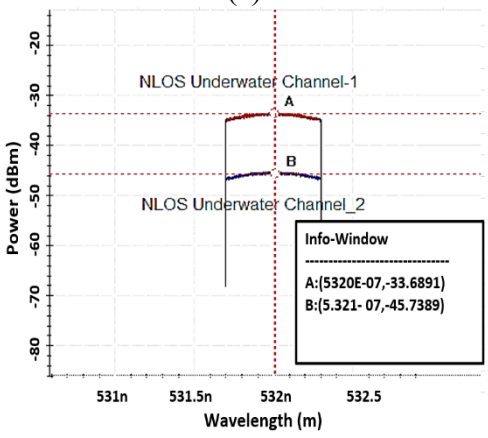

(b)

Figure 7. Variation in horizontal distance between TX and RX concerning platform depth is depicted in Figure (a), whereas Figure (b) illustrates the received power at a constant horizontal separation of 50 meters.

The system was assessed to determine the optimal horizontal distance between the transmitter and receiver, with platform separation extending up to a maximum of 90 meters, as illustrated in Figure 7(a). The lowest BER was observed at approximately 50 meters, which aligns well with the theoretical calculations presented earlier.

Figure 7(b) shows the power received by the two platforms, each measuring –33.6 dBm and –45.7 dBm, at a depth equal to 20 m, with the transmitter and receiver spaced equal to 50 m apart horizontally.

The supposed maximum angle at which the receiver can detect dispersed light is called the outer angle, or θ_{max}. The amount of scattered light that the receiver can pick up depends on this angle. Snell's Law formula can also be used to determine the critical angle θ_c in Figure 10: By using the refractive index of water (n_1=1.33) and the refractive index of air (n_2=1).

$$\theta c = \text{arcsine}\ (n2/\ n1) \quad (8)$$

If the signal is incident at an angle larger than the critical value, approximately 48.6 degrees, total internal reflection occurs, as explained in Figure 8, which describes that the signal between the two platforms remains undetected till the incidence angle exceeds the critical angle.

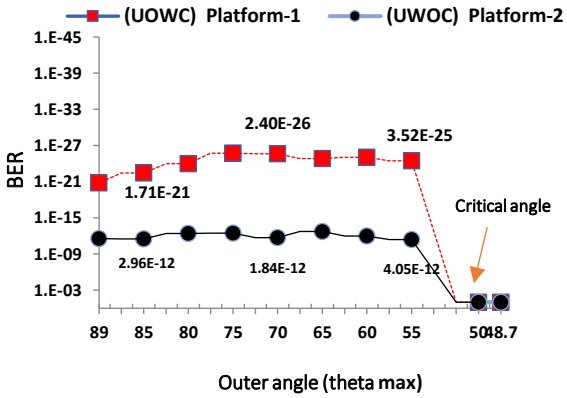

Figure 8. Outer Angle (θ_{max}) of Two Platforms Relative to the Critical Angle

The determined eye diagram at specific points on the individual curve illustrates the performance of both systems, showing that the signal is closely absent near the critical point's influence region. The maximum angle determining the allowable error rate is approximately 89°. As a final step, the system will be tested using the extracted parameters to evaluate the maximum transmit and receive depths achievable by both platforms.

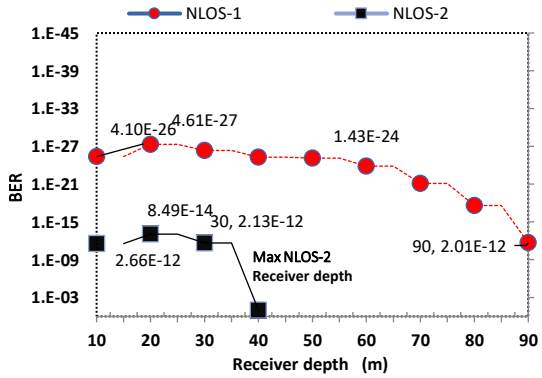

Figure 9. Highest depth reached for two platforms

As seen in Figure 9, the first platform continues to function up to almost 90 m, but the second platform's maximum depth is restricted to about 30 m because the signal almost stops at 40 m.

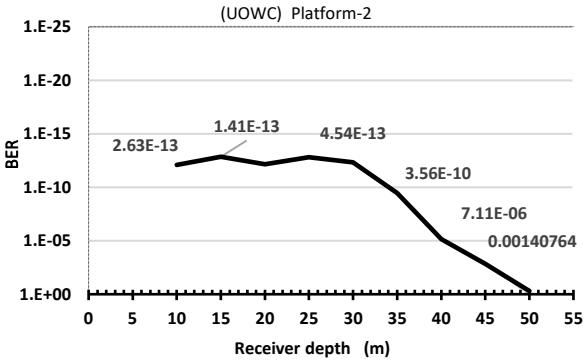

Figure 10. Highlighting the effect of the first platform's depth of 40 meters on the second

To highlight the impact of the first platform's 40-meter depth on the second platform, which led to the second platform's decommissioning, Figure 10 shows that the first platform's depth was fixed at 40 meters, while the second platform's depth varied from 5 meters to 50 meters. It was noted that the second platform's performance remained acceptable between depths of 5 and 35 meters, BER equal to 7.11×10^{-6}.

These observations allow for the deduction of the following conclusions: The performance of the second platform suffers when the NLOS-1 platform's depth is increased. As was previously mentioned, elements like depths and angles define the restrictions observed in the results. Both Figures 6 and 7 prove the effect of attenuation settings on the signal strength that is received by the underwater station. To reduce the disadvantages of the effects, the signal generated from the terrestrial link was improved by incorporating an Erbium-Doped Fiber Amplifier (EDFA), which enhanced both the flexibility and range of the FSO-2 system, resulting in a notable increase in underwater signal strength. To highlight the importance of these results, Table 6 provides a qualitative investigation for this study compared to the recent related studies, focusing on performance indicators such as the quality factor, system implementation, and use of amplification technique.

Table 6. Evaluation of the suggested Work with Current Related Works

Ref.	System setting	Signal amplification technique	achieved-factor	Notes
This study	Hybrid terrestrial FSO/fiber channels/FSO-2 to UOWC platform	EDFA in a terrestrial FSO link	Improved from 16.18 to 60.06	Signal received with gain (29.5 – 5.48) dBm
[40]	Multi-hop RF/FSO/UOWC with decode-forward (DF) relay	No EDFA; models fading in FSO/UOWC channels	N/A	Emphasizes theoretical analysis of outage probability, bit error rate, and capacity rather than practical end-to-end system performance metrics
[41]	300 GHz FSO with hybrid OQPSK/AM modulation	No EDFA; examines extreme weather	N/A	Terrestrial FSO only; aims to mitigate attenuation in rain/fog
[42]	Bidirectional FSO-5G link at 1–10 Gb/s over 1.6 km	High-power EDFA cascade	N/A	Focus on integrating FSO with 5G, not UOWC

The table above highlights that the suggested technique is among the first to demonstrate a hybrid terrestrial FSO to NLOS UOWC system incorporating an EDFA for signal amplification. This approach extends the range of bidirectional FSO communication while maintaining ultra-low BER in underwater optical wireless communication. Furthermore, the work contributes to bridging the gap between terrestrial amplifier technologies and underwater communication deployments.

4. CONCLUSIONS

This study has successfully demonstrated the design and performance evaluation of a hybrid optical communication system that bridges terrestrial Free-Space Optical (FSO) links with underwater optical connectivity. By integrating direct fiber optic cables with FSO channels and incorporating an Erbium-Doped Fiber Amplifier (EDFA), the proposed system effectively mitigates signal attenuation challenges arising from environmental conditions and medium transitions. Beyond proving the technical feasibility, the findings highlight the system's capability to sustain reliable high-speed data transmission across air–water interfaces, with significant improvements in signal quality and extended operational ranges. Notably, the enhancement of terrestrial link performance through the EDFA had a direct and measurable impact on underwater communication reliability, enabling Non-Line-of-Sight (NLOS) platforms to achieve depths and distances previously unattainable using conventional methods.

This work underscores the importance of a holistic system-level approach when addressing hybrid

communication challenges, particularly in scenarios where cross-medium propagation and variable environmental factors are critical constraints. While the results are promising, further research is warranted to explore adaptive alignment techniques and scalable deployment strategies for dynamic marine environments.

Ultimately, this study provides a foundational step toward practical hybrid terrestrial–underwater optical communication networks, offering valuable insights for future applications in underwater exploration, environmental monitoring, and defense communications. Improvements in the terrestrial network infrastructure, particularly through the integration of optical amplification, had a direct and positive impact on the performance of the underwater optical wireless communication (UOWC) link, including Non-Line-of-Sight (NLOS) scenarios. These enhancements extended the transmission range and depth, enabling the first NLOS underwater platform to operate at depths exceeding 90 meters, while the second platform achieved reliable communication over distances up to 40 kilometers. Additionally, the deployment of a 20-meter-deep optical fiber connection, exhibiting a low attenuation of 0.2 dB/km, provided a stable and efficient alternative to conventional UOWC Line-of-Sight (LOS) links. This fiber-based approach not only reduced signal degradation but also minimized alignment challenges, making it a practical solution for complex underwater environments where direct optical paths are not feasible. While this study primarily focused on system implementation and performance evaluation using OptiSystem simulations, we recognize that deeper analytical investigations are essential to further strengthen the scientific rigor of the proposed hybrid communication link. Future work will extend this research by incorporating detailed parametric analyses, advanced channel modelling, and sensitivity studies under diverse environmental conditions. Additionally, exploring adaptive alignment and dynamic compensation techniques will be critical to enhancing system robustness and practical deployment in complex real-world scenarios.

References

[1] M. M. Zayed and M. Shokair, “Performance analysis and optimization of modulation techniques for underwater optical wireless communication in varied aquatic environments,” Sci Rep, vol. 15, no. 1, p. 32570, 2025.

[2] A. Krishnamoorthy et al., “Optical Wireless Communications: Enabling the Next-Generation Network of Networks,” IEEE Vehicular Technology Magazine, vol. 20, no. 2, pp. 20–39, 2025, doi: 10.1109/MVT.2025.3555366.

[3] M. M. Zayed and M. Shokair, “Modeling and simulation of optical wireless communication channels in IoUT considering water types turbulence and transmitter selection,” Sci Rep, vol. 15, no. 1, p. 28381, 2025.

[4] J. Li et al., “NLOS Underwater Optical Wireless Communications with Wavy Surface Using Relay Coordination Based on Incremental Hybrid Decode-Amplify-Forward Scheme,” Journal of Lightwave Technology, 2025.

[5] D. Palaić, N. Lopac, I. Jurdana, and D. Brdar, “Advancements and challenges in underwater wireless optical communication in the marine environment,” in 2024 47th MIPRO ICT and Electronics Convention (MIPRO), 2024, pp. 1760–1765.

[6] Z. Li, W. Li, K. Sun, D. Fan, and W. Cui, “Recent Progress on Underwater Wireless Communication Methods and Applications,” J Mar Sci Eng, vol. 13, no. 8, p. 1505, 2025.

[7] D. Sharma, A. Tripathi, and M. Kumari, “FSO systems for next generation networks: a review, techniques and challenges,” Journal of Optical Communications, vol. 45, no. s1, pp. s1005–s1019, 2025.

[8] V. V Belgaonkar, R. Sundaraguru, and C. Poongothai, “Enhancing Free Space Optical System Performance through Fog and Atmospheric Turbulence using Power Optimization,” Engineering, Technology & Applied Science Research, vol. 15, no. 1, pp. 19390–19395, 2025.

[9] S. P. Singh, S. K. Shrivastava, S. Sengar, and S. Nath, “Fiberless optical communication: issues and challenges,” Journal of Optical Communications, vol. 45, no. s1, pp. s1179–s1200, 2025.

[10] M. M. Zayed and M. Shokair, “Performance analysis of 450/520 nm LD-PS based UOWC systems for IoUT applications across various water conditions using opti-system,” Opt Rev, pp. 1–21, 2025.

[11] N. A. Hamdullah and M. Çevik, “A Review on Underwater Optical Wireless Communication (UOWC) Technology: Current Trends and Future Prospects,” in 2025 7th International Congress on Human-Computer Interaction, Optimization and Robotic Applications (ICHORA), 2025, pp. 1–8.

[12] Z. Liu et al., “Advances in Laser Linewidth Measurement Techniques: A Comprehensive Review,” Micromachines (Basel), vol. 16, no. 9, p. 990, 2025.

[13] F. K. Shakir, M. A. A. Ali, and S. K. Rahi, “Enhancement of free-space optical communication in fog conditions with wavelength division multiplexing technique,” Journal of Optics, pp. 1–8, 2025.

[14] R. Saiyyed, M. Sindhwani, B. Ambudkar, S. Sachdeva, A. Kumar, and M. K. Shukla, “Free space optical communication system: A review of practical constraints, applications, and challenges,” Journal of Optical Communications, vol. 46, no. 2, pp. 357–363, 2025.

[15] S. Bibi, M. I. Baig, F. Qamar, and R. Shahzadi, “A comprehensive survey of free-space optical communication–modulation schemes, advantages, challenges and mitigations,” Journal of Optical Communications, vol. 45, no. s1, pp. s2373–s2385, 2025.

[16] S. Kaur, A. Sharma, and A. Sharma, “Characterization of FSO link performance considering weak to high turbulence conditions,” Journal of Optical Communications, 2025.

[17] H. Wen, H. Yin, X. Ji, and A. Huang, “Modeling and performance analysis of underwater wireless optical absorption, scattering, and turbulence channels employing Monte Carlo-multiple phase screens,” Appl Opt, vol. 62, no. 26, pp. 6883–6891, 2023, doi: 10.1364/AO.498451.

[18] B. C. AK, A. Biju, A. Bothra, D. Sarkar, and S. K. Sahu, "Modeling the Impulse Response of an Underwater Wireless Optical Communication System," in 2024 International Conference on Recent Advances in Electrical, Electronics, Ubiquitous Communication, and Computational Intelligence (RAEEUCCI), 2024, pp. 1–5.

[19] S. Li et al., "Breakthrough Underwater Physical Environment Limitations on Optical Information Representations: An Overview and Suggestions," J Mar Sci Eng, vol. 12, no. 7, 2024, doi: 10.3390/jmse12071055.

[20] A. S. Abrar and M. S. D. Rani, "Underwater visible light communication: recent advancements and channel modeling," Journal of Optics, 2025, doi: 10.1007/s12596-025-02839-9.

[21] J. M. Barraza-Contreras, M. R. Piña-Monárrez, M. M. Hernández-Ramos, and S. Ramos-Lozano, "Weibull Reliability Based on Random Vibration Performance for Fiber Optic Connectors," Vibration, vol. 8, no. 3, p. 46, 2025.

[22] Y. Gao et al., "Experimental study of subcarrier intensity modulation schemes for underwater wireless optical communication in turbulence channels," Optical Engineering, vol. 64, no. 5, p. 58105, 2025.

[23] S. H. Alnajjar, M. H. Ali, and A. ~K. Abass, "Enhancing Performance of Hybrid FSO/Fiber Optic Communication Link Utilizing Multi-Channel Configuration," Journal of Optical Communications, vol. 43, no. 1, pp. 165–170, Jan. 2022, doi: 10.1515/joc-2018-0193.

[24] I. I. Kim, B. McArthur, and E. J. Korevaar, "Comparison of laser beam propagation at 785 nm and 1550 nm in fog and haze for optical wireless communications," in Proc.SPIE, Feb. 2001, pp. 26–37. doi: 10.1117/12.417512.

[25] S. J. Rajput and Y. B. Acharya, "Performance Analysis of 25 Gbps DP-QPSK Based Co-OFDM-FSO Link Incorporating Spatial Diversity Under Climate Conditions and Atmospheric Turbulence," Progress in Electromagnetics Research C, vol. 133, 2023.

[26] S. H. Alnajjar, A. A. Noori, and A. A. Moosa, "Enhancement of FSO communications links under complex environment," Photonic sensors, vol. 7, no. 2, pp. 113–122, 2017.

[27] S. H. Alnajjar and B. K. Al Faris, "Performance Analysis of Optical-CDMA via FSO effect on Li-Fi system utilizing L'Band frequencies," in 2022 5th International Conference on Information and Communications Technology (ICOIACT), 2022, pp. 48–53. doi: 10.1109/ICOIACT55506.2022.9972175.

[28] O. Bouchet, H. Sizun, C. Boisrobert, and F. De Fornel, Free-space optics: propagation and communication, vol. 91. John Wiley & Sons, 2010.

[29] S. H. Alnajjar and B. K. ALfaris, "OCDMA performance on FSO turbulent weather channel on Li-Fi systems," Al-Iraqia Journal for Scientific Engineering Research, vol. 1, no. 2, pp. 1–8, 2022.

[30] R. Kaler and R. S. Kaler, "Gain and Noise figure performance of erbium doped fiber amplifiers (EDFAs) and Compact EDFAs," Optik (Stuttg), vol. 122, no. 5, pp. 440–443, 2011.

[31] A. A. B. Raj et al., "A Review–Unguided Optical Communications: Developments, Technology Evolution, and Challenges," Electronics (Basel), vol. 12, no. 8, 2023, doi: 10.3390/electronics12081922.

[32] T. Theocharidis and E. Kavallieratou, "Underwater communication technologies: a review," Telecommun Syst, vol. 88, no. 2, p. 54, 2025, doi: 10.1007/s11235-025-01279-x.

[33] S. Arya and Y. H. Chung, "A Comprehensive Survey on Optical Scattering Communications: Current Research, New Trends, and Future Vision," IEEE Communications Surveys & Tutorials, vol. 26, no. 2, pp. 1446–1477, 2024, doi: 10.1109/COMST.2023.3339371.

[34] B. R. Angara, P. Shanmugam, and C. G. Sandhani, "Evaluation of underwater optical wireless communication in the visible spectral domain," J Quant Spectrosc Radiat Transf, p. 109562, 2025.

[35] D. J. Biswas, "Behavior of Light," in A Beginner's Guide to Lasers and Their Applications, Part 1: Insights into Laser Science, D. J. Biswas, Ed., Cham: Springer International Publishing, 2023, pp. 15–57. doi: 10.1007/978-3-031-24330-1_2.

[36] S. A. Abd El-Mottaleb, M. Singh, A. Atieh, and M. H. Aly, "High data rate underwater optical wireless communication systems with ICSM codes within green spectrum," Opt Quantum Electron, vol. 57, no. 4, p. 213, 2025, doi: 10.1007/s11082-025-08065-8.

[37] N. Payal and D. S. Gurjar, "Hybrid FSO/RF and UWOC system for enabling terrestrial–underwater communication: Performance analysis," Physical Communication, vol. 68, p. 102540, 2025, doi: https://doi.org/10.1016/j.phycom.2024.102540.

[38] Y. Chen, H. Qiu, and Y. Li, "Research on Rate Adaptation of Underwater Optical Communication with Joint Control of Photoelectric Domain," Photonics, vol. 11, no. 11, 2024, doi: 10.3390/photonics11111004.

[39] Y. Ata and K. Kiasaleh, "Analysis of Optical Wireless Communication Links in Turbulent Underwater Channels With Wide Range of Water Parameters," IEEE Trans Veh Technol, vol. 72, no. 5, pp. 6363–6374, 2023, doi: 10.1109/TVT.2023.3235823.

[40] H. H. Alhashim et al., "An Insight to the Outage Performance of Multi-Hop Mixed RF/FSO/UWOC System," Photonics, vol. 10, no. 9, 2023, doi: 10.3390/photonics10091010.

[41] R. Z. Yousif, "Improved 300 GHz FSO communication link performance using hybrid OQPSK/AM modulation with predistortion under extreme weather conditions," Opt Quantum Electron, vol. 55, no. 7, p. 649, 2023, doi: 10.1007/s11082-023-04951-1.

[42] S. T. Hayle et al., "High-speed FSO-5G wireless communication system with enhanced loss compensation using high-power EDFA," Sci Rep, vol. 15, no. 1, p. 379, 2025, doi: 10.1038/s41598-024-84436-7.